NUMERICAL INVESTIGATION OF THE BLAST PERFORMANCE OF REINFORCED CONCRETE COLUMNS SUBJECTED TO CLOSE-IN EXPLOSION

Ben Rhouma, Mohamed; Aminou , Aldjabar; Maazoun, Azer; Belkassem, Bachir; Tysmans, Tine; Lecompte, David

Published in:
Proceedings of the 6th International Conference on Protective Structures

Publication date:
2023

License:
Unspecified

Document Version:
Final published version

6th International Conference on Protective Structures (ICPS6)
14 – 17 May 2023, Auburn University USA

NUMERICAL INVESTIGATION OF THE BLAST PERFORMANCE OF REINFORCED CONCRETE COLUMNS SUBJECTED TO CLOSE-IN EXPLOSION

Ben Rhouma Mohamed*[a,b], Aminou Aldjabar[a,b], Maazoun Azer[C], Belkassem Bachir[a], Tine Tysmans[b], and Lecompte David[a]

[a]Royal Military Academy, Propellant Explosives and Blast Engineering Department
Avenue de la Renaissance 30, 1000 Brussels, Belgium
*e-mail: Mohamed.BenRhouma@mil.be

[b]Vrije Universiteit Brussels, Mechanics of Materials and constructions Department
Pleinlaan 2, 1050 Brussels, Belgium

[C] Military Academy of Fondouk Jedid, Civil Engineering Department, 8021 Nabeul, Tunisia

ABSTRACT

Explosive incidents, whether accidental or intentional, can lead to significant damage to buildings and potentially cause a large number of human casualties. The progressive collapse of a targeted building is one of the most devastating consequences of an explosion occurring in the vicinity. This phenomenon takes place when critical structural elements, such as reinforced concrete (RC) columns, fail due to blast loading. Therefore, this paper aims to develop a physics-based finite element model of an RC column subjected to blast loading using explicit LS-DYNA software. Two methods are compared, including Load Blast Enhanced (LBE), and the pressure time history method (triangular pulse). The Karagozian & Case concrete (KCC) constitutive model is selected. The models are validated against experimentally obtained mid-span displacement time histories and damage characteristics. The results are in agreement with the test data. The influence of the explosive charge weight, stand-off distance, and column cross-section on the blast performance of RC columns and the residual axial bearing capacity are investigated. The findings provide insights into the behavior of RC columns under blast loading and can be used in the design of blast-resistant structures.

Keywords: RC column, Blast loading, Numerical modeling, LS-DYNA

distribution statement (if required)

INTRODUCTION

Intentional and accidental explosions have increased worldwide over the last two decades. In 1995, a terrorist attack on the Alfred P. Murrah building occurred leading to 268 deaths and severe damage to the nearby buildings. The blast loading was generated by the explosion of a Vehicle-Borne Improvised Explosive Device (VBIED) containing around 1818 kg of equivalent TNT standing near the target. This bombing led to a shear failure in several non-redundant exterior RC columns. As a result, the other structural members were not able to redistribute the load coming from the upper portion of the structure. Hence, that blast-induced structural instability resulted in a cascading collapse in a large portion of the building [1]. This example shows the degree of damage related to the failure of axial bearing members and the important number of fatalities due to terrorist attacks and accidental explosions.

So, the major focus of the researchers has shifted from assessing the response of reinforced concrete (later on referred to as RC) columns under conventional loads such as gravity and seismic to evaluating its dynamic behavior under different blast events. Several studies have been carried out to investigate the dynamic behavior of RC columns under distant and close-in explosions. Initially, an explosion could be classified as a close-in blast event when the scaled distance $z < 1.054$ kg/m$^{1/3}$ [2] or $z < 1.2$ kg/m$^{1/3}$[3][4]. The scaled distance Z is equal to $R/W^{1/3}$, where R is the stand-off distance or the distance between the center of the explosive charge and the structure and W defines the explosive mass. Considering the close-in event, some researchers have carried out experiments to assess the effects of blast and column-related parameters on the dynamic response of RC columns. Woodson et al. [14] carried out five experiments on quarter-scale RC columns included in scaled two-story RC frames under close-in explosion. The test specimens were characterized with a cross-section of 89 x 89 mm² and a 935 mm height. A hemispherical C-4 charge of 7.1 kg was placed 229 mm above the ground and at a stand-off distance of 1520 mm and 1070 mm facing the nearest exterior RC column. It was concluded that increasing the scaled distance leads to lesser damage to the test columns. The influence of the scaled distance, and detailing of RC columns were experimentally investigated by Braimah et al [5]. Sixteen full-scale conventional and seismically detailed RC columns were designed according to the Canadian code CSA A23.3-14. Both columns had a cross-section of 300 mm x 300 mm and a 3200 mm height. The specimens were subjected to the close-in explosion of 100 kg and 150 kg of ANFO situated at 1100 mm, 2700 mm, and 4300 mm. Compared to conventional RC columns, structural members detailed for seismic resistance exhibited higher blast bearing capacity in the case of the close-in explosion. However, due to the shortage of testing sites and safety reasons concerning the hazards associated with blast tests, and with the current developments in computer programs, it becomes possible to model RC columns under a given blast scenario and validate the numerical results against test data. For instance, the experimental results cited in [6] have been used by several authors [9,10,15-17] to validate their numerical models and perform parametric studies using the physics-based explicit LS-DYNA. It is proved that parameters such as concrete strength [7], column's detailing[8–12], column's dimensions [13], column's shape [10,14] and axial load ratio[10,15,16], play an important role in the damage degree of the RC structural member. Besides, the effects of the explosive mass, shape and scaled distance on the anti-blast performance and deformation modes of the columns are also assessed [17,18]. In previous study, the effects of the column's shape on the residual strength of the blast damaged load bearing member have not been performed. Therefore, the objective of this work is to address such a gap in literature.

The present paper is divided into five parts. Firstly, a brief description of the adopted experiment is presented along with the steps followed to develop the finite element model of the corresponding benchmark. Secondly, the numerical results are compared to the available test data and validated. In the third and fourth parts, the effects of key parameters on the mid-span displacement and residual axial strength of square and equivalent circular RC columns are analyzed and discussed, respectively. Finally, conclusions and perspectives on future work are given.

FINITE ELEMENT MODELING OF THE EXPERIMENTAL SET-UP

Experimental blast test

The second experiment of Woodson et al. [6] is adopted to validate the current numerical model based on the response of the central column shown in **Figure 1.**

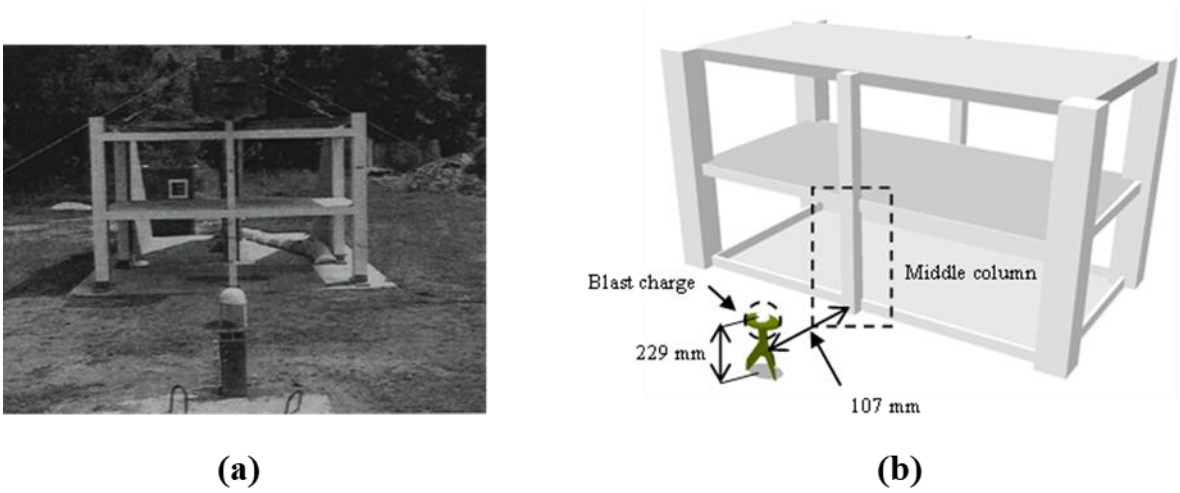

Figure 1. (a) Experimental setup developed by Woodson et al. (b) Sketch of the experimental model showing the placement of the explosive charge with respect to the middle column.

FE modeling of the experimental benchmark

At first, the finite element modeling of the tested exterior column is performed. Details about the numerical model are included in **Figure 2.** b represents the column width; d is the column depth and a is the concrete cover sets as 9.5mm. h is the clear height of the column and s is the spacing of the ties. The cross-section of the column is 85mm x 85mm with 8 longitudinal reinforcements of Ø = 7.1 mm. The height of the model is 935 mm with a transverse reinforcement of Ø = 3.85 mm spaced at 89 mm. 8-node constant stress solid elements with 1-point quadrature integration are adopted to model the concrete while 2-node Hughes-Liu beam element with 2 x 2 Gauss quadrature integration is chosen for the steel reinforcements. A numerical convergence study is carried out by halving the mesh size. Further decrease of the mesh size has only an insignificant influence on the numerical results but can result in undesirable memory overflow. Therefore, a 10 mm mesh is used in the numerical model. In this study, the column is constrained at the footing and head to prevent any translational movement (x, y-directions), and the bottom face is also fixed to prevent vertical motion in the z-direction. Top nodes are not constrained along the column axis to allow axial load. To prevent zero-energy modes, The Flanagan-Belytschko stiffness form of the hourglass control keyword is used during the simulations. The hourglass coefficient of 0.1 is adopted for the reduced integration elements[10]. An axial load of 2.1 MPa was applied at the top of the RC column to represent the gravity load coming from the structural framing before applying later blast loading to the column's front face.
The three-dimensional (3-D) finite element model comprises the following parts as illustrated in **Figure 2**:

1- The concrete column;
2- The longitudinal and transverse rebars;
3- The axial load.

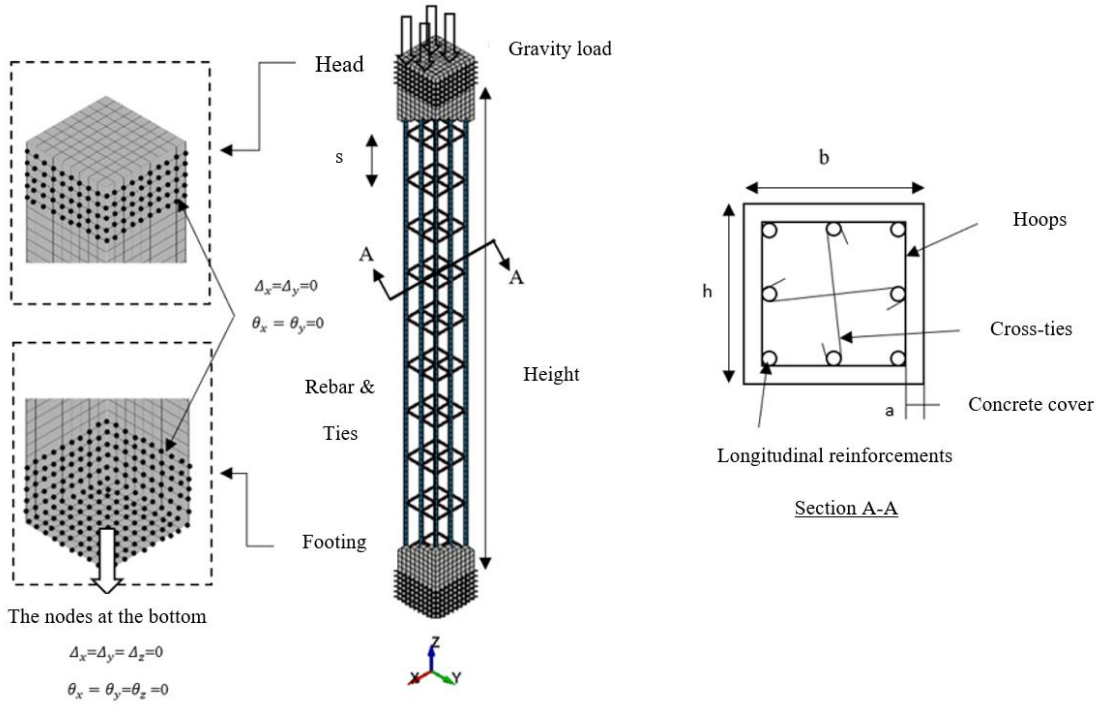

Figure 2. Boundary conditions of the calibration model for RC column

The choice of the constitutive models is important to reliably predict the behavior of RC members under a given blast event.

Concrete constitutive model

Several constitutive models included in LS-DYNA can be adopted for concrete, such as the Karagozian & Case (KCC or CONCRETE DAMAGE REL3), the Winfrith model (WINFRITH-CONCRETE), and the CSCM model (CONTINUOUS SURFACE CAP MODEL). Each of the aforementioned models has its advantages and limitations.

The *MAT 072R3 was created to analyze the behavior of RC structural elements to blast and impact loadings. It was first implemented in LS-DYNA in 2004 [19]. It has been adopted to present the concrete model included in RC structural elements subjected to blast loading [20–25]. Compared to *MAT_WINFRITH_CONCRETE and *MAT_CSCM_CONCRETE, this model has proven its efficiencies in generating the concrete's aspects and behavior under extreme loading cases such as blast loading (i.e., non-linear hardening and softening, shear dilation, confinement effect) [26]. Besides, this model is able of generating automatically all parameters related to concrete only by inserting the unconfined compressive strength and the density of strength [24,27,28].

The default parameters of the model are determined based on large test data aiming to calibrate the concrete response[19].The input parameters for the concrete model are presented in **Table 1.**

The concrete element will be numerically erased if the principal maximum strain is equal to 0.1 defined in *MAT_ADD_EROSION card [29]. The KCC model is sensitive to mesh size. The default generated parameters are only valid for an element size of 25.4 mm. Since the mesh size is chosen 10 mm based on the convergence study, an adequate calibration is to be conducted mainly to three parameters which are ω, B_1, and B_2. Those inputs define the volume expansion, the compressive damage evolution, and the tensile damage evolution, respectively. The analytical expressions used to calculate these parameters are cited in [22,30].

Table 1. Static material properties for the KCC material model.

Parameter	value
Mass density, (kg/m^3)	2068
Uniaxial compressive strength, (MPa)	42
Poisson's Ratio	0.3

Reinforcement constitutive model

The *Piecewise_Linear_Plasticity MAT024 model is an elasto-plastic material in which the engineering stress-strain curve for a selected material can be defined. Besides, this model can include an arbitrary strain rate curve in addition to the Cowper Symond rate enhancement which is its main feature. This latter option allows us to attain more accurate results since the strain rate input is highly dependable on the mechanical characteristics of the selected grade for the rebars as shown in the strain rate section.
The input parameters for the rebars model are presented in **Table 2**.

Table 2: Static material parameters for steel constitutive model[31] **.**

Parameter	Longitudinal steel reinforcement	Transverse steel reinforcement
Mass density, (kg/m^3)	7800	7800
Yield strength, (MPa)	450	400
Young's modulus, (GPa)	207	207
Poisson's Ratio	0.33	0.33
Failure strain	18%	18%

Contact algorithm between steel reinforcement and concrete

The constraint between steel reinforcements and concrete elements is defined used the keyword called *CONSTRAINED-BEAM-IN-SOLID or CBIS an alternative to *CONSTRAINED-LAGRANGE-IN-SOLID or CLIS or the "shared nodes" technique which represent some numerical flaws[32].

Strain rate effects

According to Bischoff et al.[33], blast loads generally produce in most structural materials extensive strain rate values ranging from 10^2 to 10^3 sec^{-1}. So, proper formulae from open literature should be adopted to consider the enhancement of the mechanical properties of the concrete and steel. This improvement is also known as dynamic increase factor (DIF) which is defined as the ratio of dynamic to static stress for different reinforced concrete structural components. For the case of the concrete constitutive model, the expressions of Malvar and Crawford [34] along with those defined in the Comité Euro-international du Béton (CEB) 1990 [33] are chosen under tension and compression, respectively.
The stress-strain behavior of steel reinforcement is sensitive to the rate of the loading. This assumption was noticed from uniaxial tensile tests varying at each time the loading rate. The formulae cited by Malvar and Crawford [35] are used to take into account the DIF for steel.

Blast load Model

The LS-DYNA software provides users with several blast simulation methods. Among these approaches are the Load_Blast_Enhanced (LBE)[36], triangular pressure-time history [37], Multi-Material-Arbitrary-Lagrangian-Eulerian (MM-ALE)[38], and coupled MM-ALE with LBE[24]. The difference between these blast load techniques is out of the scope of this work. For our case, *LOAD_BLAST_ENHANCED (LBE) is used for numerical simulations [36,39,40]. The blast load is defined by the position of the detonation

point, and the explosive weight [41]. The LBE technique is not as time-consuming as MM-ALE or coupling LBE with MM-ALE. The reason is that this approach does not include the detonation process and the blast wave propagation in the air[42]. Hence, only the blast wave parameters will be applied to the RC column based on the scaled distance Z and the angle of incidence. The scaled distance is calculated as $Z = R/W^{1/3}$, where R is the stand-off distance and W defines the explosive mass [41]. It is worth noting that the analytical formulae of Kingery and Bulmash defining the shock wave parameters were adopted for the LBE method [19]. Moreover, the surface on which the shock front will be acting is recognized in LS-DYNA through *LOAD-BLAST-SEGMENT-SET.

For comparative reasons, the idealized triangular pressure-time history which has been used by several authors for the validation of their FE models [29,37,38] is adopted for this work. A load curve is introduced to LS-DYNA via the keyword: *DEFINE_CURVE. This equivalent triangular blast load is defined by a peak reflected pressure which decays linearly to the atmospheric pressure during the effective positive duration. This duration is calculated based on the equivalent positive reflected impulse and pressure. The *SET_SEGMENT option is used to define the surface of the RC column facing the idealized blast load. The interaction between the RC column and the triangular blast pressure is activated via *LOAD_SEGMENT_SET keyword. This blast load is applied uniformly along the height of the column.

Residual axial capacity

The approach adopted in this paper to assess the vulnerability of RC columns to axial and lateral blast loading is first cited in [9]. During the first stage, gravity loads will be applied on top of the RC column Several scholars [10,23,37,43,44] used the same methodology.

In this paper, the gravity load is applied as a uniformly distributed pressure during a dynamic relaxation analysis through the option *CONTROL_DYNAMIC_RELAXATION (referenced as phase 1 later on). Hence, the blast loading phase or the second phase is conducted when a constant stress state is reached within the RC column.

To investigate the residual axial strength, a complete restart should be done and a downward vertical displacement is applied until the column fails. The full restart is possible by retaining stress, strain, and displacements of all the nodes of the model. In LS-DYNA, this is done through *STRESS_INITIALIZATION.

RESULTS OF THE FE MODEL AND COMPARISONS

The deflection of the RC column determined by several authors in [6,10,36] is compared in this work with the results from the developed numerical model as shown in **Error! Reference source not found.** and **Error! Reference source not found.**.

The experimental lateral peak displacement is 12.63 mm while the numerical results using LBE and triangular blast pressure result in 12.48 mm and 11.82 mm, respectively. The numerical residual displacements are 6.51mm and 5.32 mm compared to the 6.5 mm experimentally measured deflection. The relative errors are calculated between the numerical results using the two blast application methods and the experimental benchmark. For the case of the LBE method, 1.2% and 0.15% are found in the maximum and residual mid-height deflection of the RC column, respectively. Besides, 6.4 % and 18% represent the relative errors between the experimental results and the numerical ones using equivalent triangular pulse. Besides, the numerical models of Rajkumar et al. [36] and Chen et al. [10] yield, relative to the experimental results, between two and ten times larger values for maximum and residual deflection, respectively.

The results show that the numerical model is in good agreement with experimental results conducted by Baylot and Bevins [31]. So, the numerical model yields good predictions of RC column blast response.

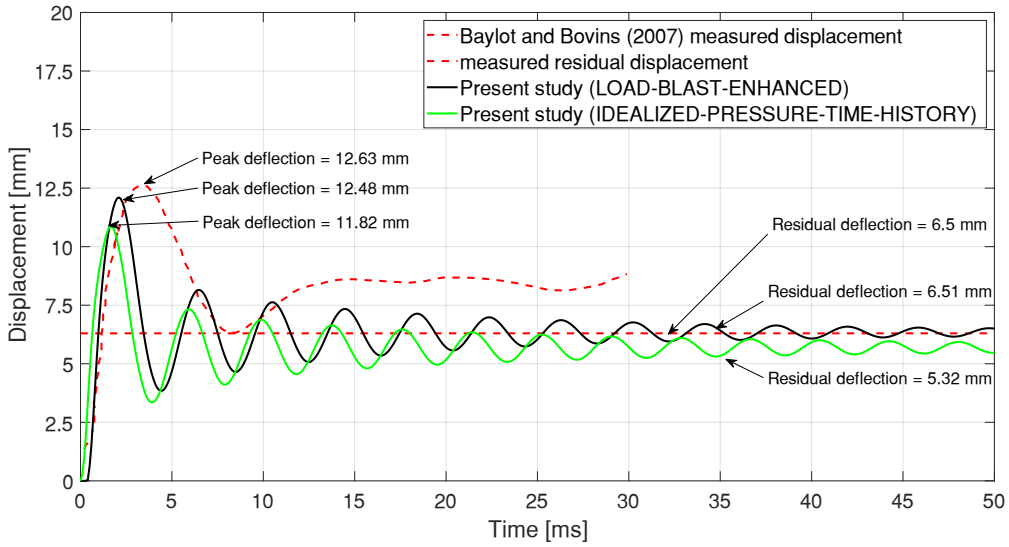

Figure 3. Comparison of the numerical deflection-time histories with respect to the results of the experimental benchmark

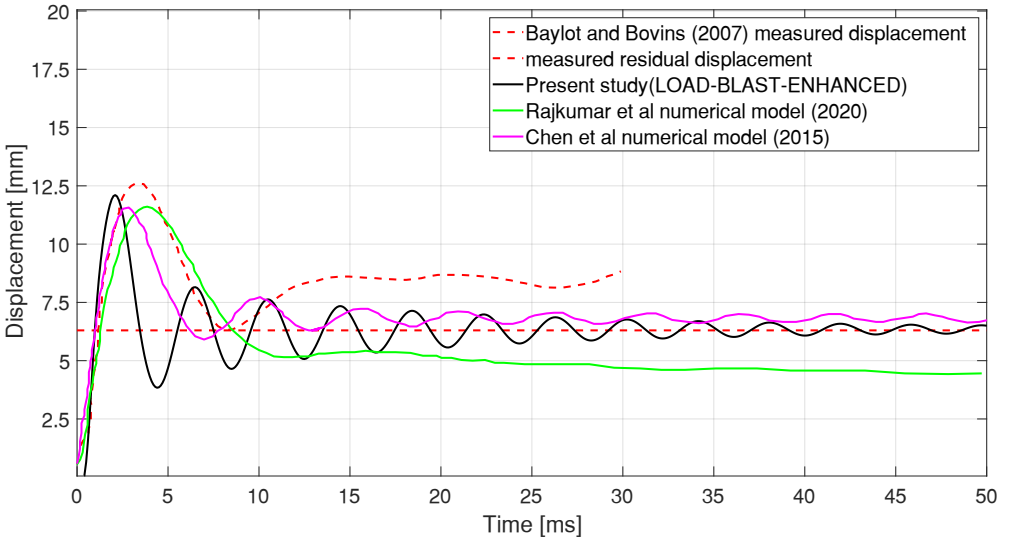

Figure 4. Comparison of deflection time-histories for different numerical mode

DISCUSSIONS ON THE EFFECT OF THE EXPLOSIVE MASS AND SCALED DISTANCE

A series of simulations are conducted to investigate the non-linear response of RC columns when varying different parameters. In this case study, the explosive charge is placed at a certain stand-off distance facing the mid-height of the RC column. The validated square RC column is considered the reference model. Therefore, the column's dimensions are kept the same as the experimental benchmark. For comparative reason, the blast performance of an equivalent circular column is also investigated. To do so, the dimensions of the equivalent column is calculated by equating the corresponding volume to that of the square member.

The number of transverse reinforcements as well as the spacing are deduced from the volumetric equivalency of reinforcements with respect to those adopted for the square column (more details are included in **Figure 5**).

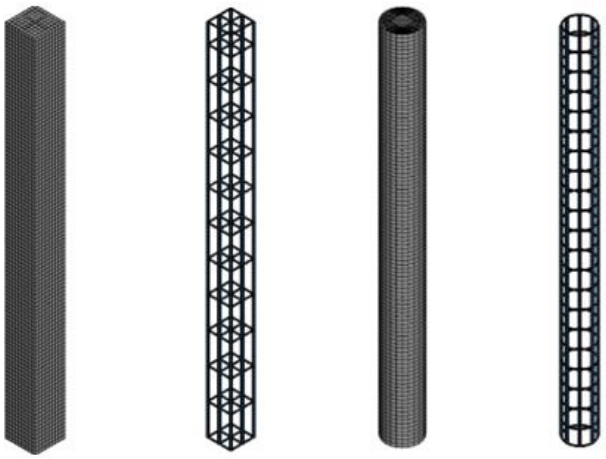

Figure 5. Detailing of the studied RC columns(a) square cross-section (b) circular cross-section

Then, their dynamic responses are quantified by comparing their lateral displacement under close-in blast loading scenarios. The influence of the explosive mass and the stand-off distance on the blast wave variables can be determined based on the scaling laws. Those laws are developed to scale parameters from the experiments to others not included in the experimental campaign by varying the explosive charge and the stand-off distance. The Hopkinson-Cranz analytical expression is the most used blast scaling law [45,46]. It cites that under the same scaled distance and atmospheric conditions, two explosive charges having the same type and geometry will produce the same peak reflected overpressure. However, for the same scaled distance, increasing the explosive charge leads to a higher reflected impulse as shown in **Figure 6.**

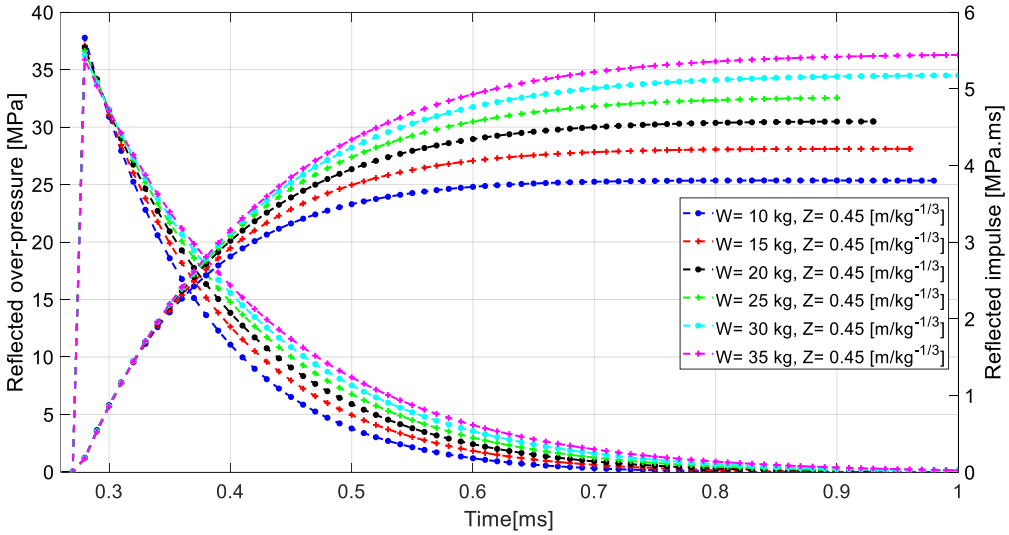

Figure 6. The influence of the explosive mass on the reflected impulse for the same scaled distance

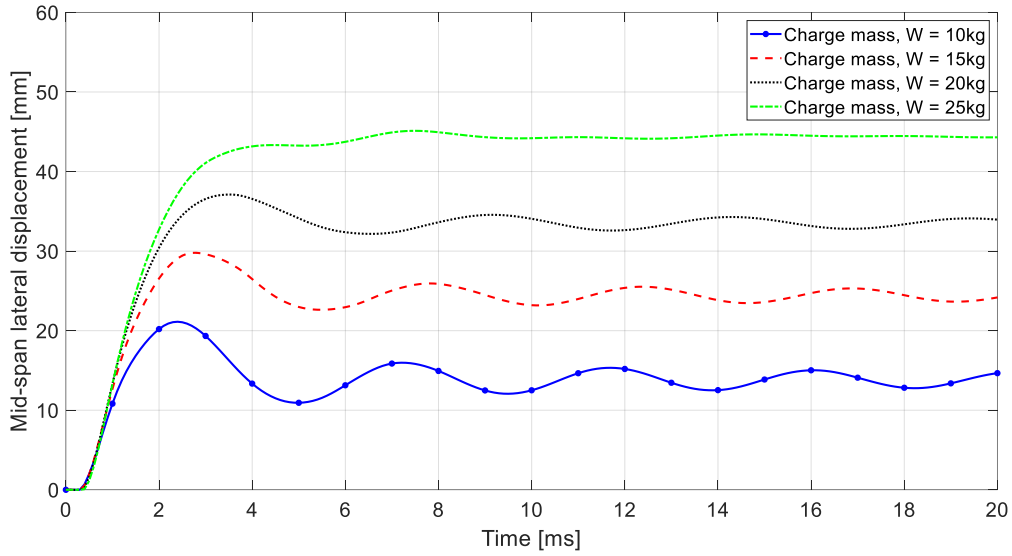

Figure 7. The effect of the explosive masses on the mid-span lateral displacement time histories for the square RC column

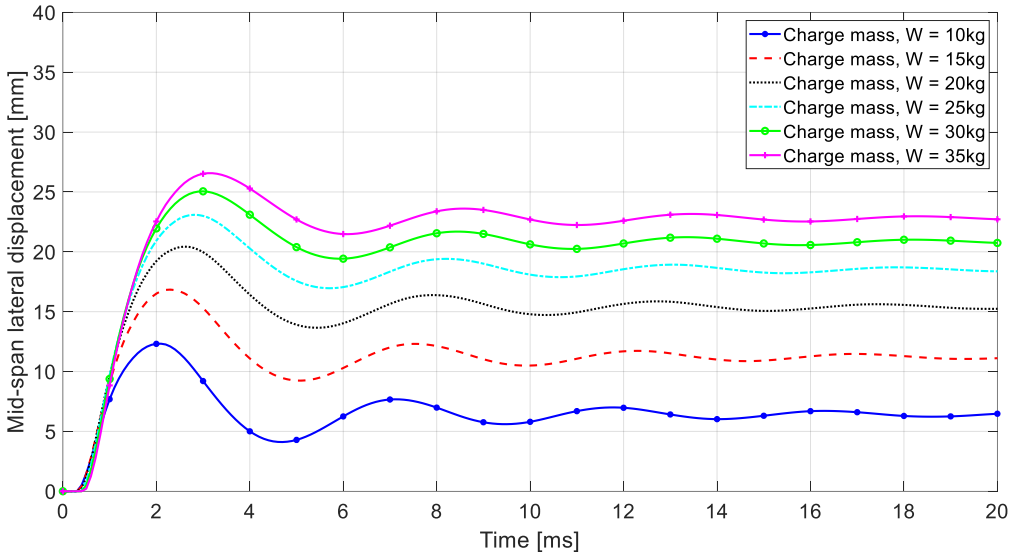

Figure 8. The effect of the explosive masses on the mid-span lateral displacement time histories for the circular RC column

Besides, as depicted in **Figure 7,** and **Figure 8,** the more the explosive charge is the larger the lateral displacement will be. Such parameter influences somehow similarly on the blast response of circular and square RC columns. However, the circular columns can sustain higher reflected impulse compared to the square ones. When the explosive mass is larger than 25 kg, square columns fail as a result of extensive damage due to the crushing and spalling of concrete as seen in **Figure 9.** The analysis of the two shapes proves that circular columns perform better under a close-in blast event. This is might be due to the effect of the circular shape on the reflected pressure and impulse. For the case of square RC column, the surface facing the blast has an infinite curvature which resulting in higher effective reflected pressure. Besides, when the scaled distance is reduced, a significant decay of reflected overpressure occurs leading to lower

blast-induced damage to the columns as seen from the results in **Figure 9** for the case of 0.5 kg/m$^{1/3}$. Those results agree well with those mentioned in [14].

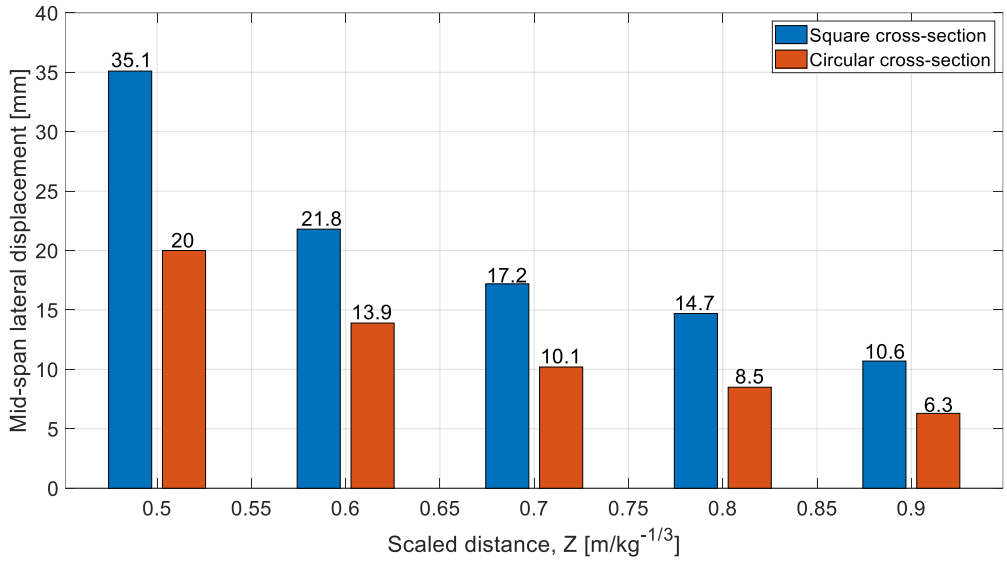

Figure 9. The evolution of the mid-span lateral displacement as a function of the scaled distance for square and circular RC columns

DISCUSSIONS ON THE DAMAGE LEVEL OF RC COLUMNS BASED ON THE RESIDUAL AXIAL STRENGTH

The damage criterion for RC columns developed by Shi et al.[9] was adopted for this work. The advantage of such method is that it can take into account both the shear and flexural damage. Compared to damage criterion developed based on the mid-span lateral displacement and cited by Fallah and Louca [47], this damage approach is more accurate.

For instance, Thai et al. [13] Hao et al. [48], Mutalib et al.[23] and Hao et al. [48], adopted the same axial force based criterion to estimate the damage level in RC columns. The damage criterion D is defined as

$$D = 1 - \frac{P_{res}}{P_{nom}} \quad (1)$$

Where P_{res} is the residual axial capacity of the blast-damaged column and P_{nom} is the nominal axial capacity of the column. The effect of the explosive mass on the residual axial capacity for selected square columns is shown in **Figure 10.** A largest residual axial force of 168 kN was recorded for the square RC column when subjected to 10 kg compared to 61 kN for a doubled explosive charge under the same scaled distance 0.45 kg/m$^{1/3}$. Under 25 kg, the square column cannot sustain its dead and live loads and fails in a brittle manner. The nominal axial force depends on the characteristics of concrete and the longitudinal reinforcements. The analytical expression (equation 1) cited in [9] is used to calculate the bearing capacity of the undamaged column. Then, based on the value of D, the damage degree of the blast loaded column is quantified (from "low" to "complete failure"). The details about the residual axial forces and the damage indices are included in **Table 3.**

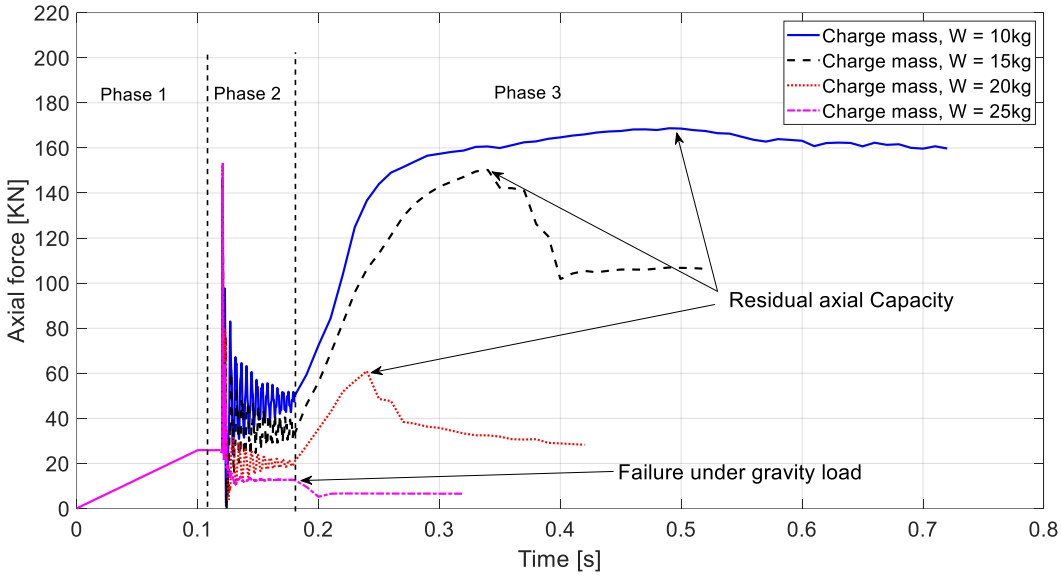

Figure 10. Axial forces as a function of time with respect to explosive masses for the case of square columns

Table 3: Blast and column-related parameters selected within this work along with axial forces and damage indices

Explosive mass	Stand-off distance (m)	Scaled distance ($m/kg^{1/3}$)	Square RC column		Circular RC column	
			Residual axial Force (kN)	Damage index	Residual axial Force (kN)	Damage index
10	0.97	0.45	168.7	0.61	172.1	0.6
15	1.11		150.2	0.65	161.4	0.63
20	1.22		60.9	0.86	153.8	0.64
25	1.32		F.D	0.9	149.2	0.65
30	1.41		F.D	0.91	145.9	0.67
35	1.47		F.D	0.95	115.1	0.73
30	1.55	0.5	124.4	0.71	152.3	0.65
	1.86	0.6	143.2	0.67	161.4	0.63
	2.18	0.7	162.1	0.63	176.1	0.59
	2.49	0.8	170.8	0.61	191.2	0.56
	2.8	0.9	188.7	0.56	201.6	0.53

* F.D: full damaged columns

CONCLUSIONS

In this paper, a nonlinear finite element model of RC column is developed and validated with experimental data available from literature. The results are in a good agreement with the test data. Parametric studies are performed on square and equivalent circular RC columns by considering the influence of the explosive mass and the scaled distance. Based on the results of the parametric study, the following conclusions are drawn:

1. Increasing the explosive mass has a great influence on the blast resistance of square RC columns. It is proved that under the same scaled distance, increasing the explosive mass could lead to brittle failure and complete loss of axial capacity to sustain service loads.
2. The numerical results quantitively proved that the circular RC columns exhibit enhanced resistance compared to square companions under close-in blast event.
3. For both square and circular columns, reducing the blast-induced damage is feasible by increasing the scaled distance.

ACKNOWLEDGMENTS

The authors are grateful to the staff of the Laboratory of Propellants, Explosives and Blast Engineering (PEBE) department of the Royal Military Academy (RMA) in Brussels for their support and assistance in performing the different steps of the experimental work.

REFERENCES

[1] Tagel-Din H, Rahman NA. Simulation of the Alfred P. Murrah federal building collapse due to blast loads. AEI 2006 Build Integr Solut - Proc 2006 Archit Eng Natl Conf 2006;2006:32. https://doi.org/10.1061/40798(190)32.

[2] Gel'fand BE, Voskoboinikov IM, Khomik S V. Recording the Position of a Blast-Wave Front in Air. Combust Explos Shock Waves 2004;40:734–6. https://doi.org/10.1023/B:CESW.0000048281.33696.ed.

[3] Enstock LK, Smith PD. Measurement of impulse from the close-in explosion of doped charges using a pendulum. Int J Impact Eng 2007;34:487–94. https://doi.org/https://doi.org/10.1016/j.ijimpeng.2005.12.005.

[4] Engineers ASC. Blast Protection of Buildings: Standard Asce/Sei 59-11. American Society of Civil Engineers; 2011.

[5] Braimah A, Siba F. Near-Field Explosion Effects on Reinforced Concrete Columns: An Experimental Investigation. Can J Civ Eng 2015;45:289–303.

[6] Woodson SC, Baylot JT. Structural Collapse: Quarter-Scale Model Experiments 1999:176.

[7] Aoude H, Dagenais FP, Burrell RP, Saatcioglu M. Behavior of ultra-high performance fiber reinforced concrete columns under blast loading. Int J Impact Eng 2015;80:185–202. https://doi.org/10.1016/j.ijimpeng.2015.02.006.

[8] Fujikake K, Aemlaor P. Damage of reinforced concrete columns under demolition blasting. Eng Struct 2013;55:116–25. https://doi.org/10.1016/j.engstruct.2011.08.038.

[9] Shi Y, Hao H, Li ZX. Numerical derivation of pressure-impulse diagrams for prediction of RC column damage to blast loads. Int J Impact Eng 2008;35:1213–27. https://doi.org/10.1016/j.ijimpeng.2007.09.001.

[10] Chen L, Hu Y, Ren H, Xiang H, Zhai C, Fang Q. Performances of the RC column under close-in explosion induced by the double-end-initiation explosive cylinder. Int J Impact Eng 2019;132. https://doi.org/10.1016/j.ijimpeng.2019.103326.
[11] Kwaffo I, Hussein Abdallah M, Braimah A. Experimental assessment of the residual capacity of axially loaded blast-damaged square RC columns. Structures 2022;40:469–84. https://doi.org/10.1016/j.istruc.2022.04.034.
[12] Kyei C, Braimah A. Effects of transverse reinforcement spacing on the response of reinforced concrete columns subjected to blast loading. Eng Struct 2017;142:148–64. https://doi.org/10.1016/j.engstruct.2017.03.044.
[13] Thai DK, Kim SE. Numerical investigation of the damage of RC members subjected to blast loading. Eng Fail Anal 2018;92:350–67. https://doi.org/10.1016/j.engfailanal.2018.06.001.
[14] N.P. P, V.G K. Effects of different reinforcement schemes and column shapes on the response of reinforced concrete columns subjected to blast loading. Int Res J Eng Technol 2018;05:571–81. https://doi.org/10.1016/j.engstruct.2017.03.044.
[15] Astarlioglu S, Krauthammer T, Morency D, Tran TP. Behavior of reinforced concrete columns under combined effects of axial and blast-induced transverse loads. Eng Struct 2013;55:26–34. https://doi.org/10.1016/j.engstruct.2012.12.040.
[16] Bao X, Li B. Residual strength of blast damaged reinforced concrete columns. Int J Impact Eng 2010;37:295–308. https://doi.org/10.1016/j.ijimpeng.2009.04.003.
[17] Liu Y, Yan J bo, Huang F lei. Behavior of reinforced concrete beams and columns subjected to blast loading. Def Technol 2018;14:550–9. https://doi.org/10.1016/j.dt.2018.07.026.
[18] Shi Y, Hao H, Li ZX. Numerical simulation of blast wave interaction with structure columns. Shock Waves 2007;17:113–33. https://doi.org/10.1007/s00193-007-0099-5.
[19] Livermore Software Technology Corporation. LS-DYNA - Keyword User's Manual, Version 970. vol. I. 2003.
[20] Dua A, Braimah A, Kumar M. Experimental and numerical investigation of rectangular reinforced concrete columns under contact explosion effects. Eng Struct 2020;205. https://doi.org/10.1016/j.engstruct.2019.109891.
[21] Alok D, Abass B, Manish K. Contact explosion response of reinforced concrete columns: Experimental and validation of numerical model. 6th Int Disaster Mitig Spec Conf 2018, Held as Part Can Soc Civ Eng Annu Conf 2018 2018:60–9.
[22] Wu Y, Crawford JE, Lan S, Magallanes JM. Validation Studies for Concrete Constitutive Models with Blast Test Data. 13th Int LS-DYNA Users Conf 2014:1–12.
[23] Mutalib AA, Hao H. Development of P-I diagrams for FRP strengthened RC columns. Int J Impact Eng 2011;38:290–304. https://doi.org/10.1016/j.ijimpeng.2010.10.029.
[24] Shuaib M, Daoud OMA, Daoud O. Numerical Analysis of RC Slab under Blast Loads Using The Coupling of LBE and ALE Method in LS-DYNA Production and Properties of HSC in Sudan View project Development of Self Compacting Concrete in Sudan View project NUMERICAL ANALYSIS OF RC SLAB UNDER BL 2016.
[25] Maazoun A, Matthys S, Atoui O, Belkassem B, Lecompte D. Finite element modelling of RC slabs retrofitted with CFRP strips under blast loading. Eng Struct 2022;252:113597. https://doi.org/10.1016/j.engstruct.2021.113597.
[26] Wu Y, Crawford JE, Magallanes JM. Concrete Constitutive Models. 12th Int LS-DYNA Users Conf 2012:1–14.
[27] Maazoun A, Matthys S, Belkassem B, Lecompte D, Vantomme J. Blast response of retrofitted reinforced concrete hollow core slabs under a close distance explosion. Eng Struct 2019;191:447–59. https://doi.org/10.1016/j.engstruct.2019.04.068.

[28] Crawford JE, Wu Y, Choi H-J, Magallanes JM, Lan S. USE AND VALIDATION OF THE RELEASE III K&C CONCRETE MATERIAL MODEL IN LS-DYNA. Transp Res Rec 2006;372.
[29] Chen W, Hao H, Chen S. Numerical analysis of prestressed reinforced concrete beam subjected to blast loading. Mater Des 2015;65:662–74. https://doi.org/10.1016/j.matdes.2014.09.033.
[30] Zhang F, Wu C, Wang H, Zhou Y. Numerical simulation of concrete filled steel tube columns against BLAST loads. Thin-Walled Struct 2015;92:82–92. https://doi.org/10.1016/j.tws.2015.02.020.
[31] Baylot JT, Bevins TL. Effect of responding and failing structural components on the airblast pressures and loads on and inside of the structure. Comput Struct 2007;85:891–910. https://doi.org/10.1016/j.compstruc.2007.01.001.
[32] Hao C. An Introduction to *CONSTRAINED_BEAM_IN_SOLID. vol. 1. 2018.
[33] BISHOFF P., PERRY SH. Compressive behaviour of concrete at high strain rates. Mater Struct 1991:425–50.
[34] L. Javier M, C. Allen R. Review of Strain Rate Effects for Concrete in Tension. ACI Mater J 2017;153:846–56. https://doi.org/10.1016/j.conbuildmat.2017.07.168.
[35] Malvar LJ, Crawford JE. Dynamic Increase Factors for Steel Reinforcing Bars. Proc Twenty-Eighth DoD Explos Saf Semin 1998:1–18.
[36] Rajkumar D, Senthil R, Bala Murali Kumar B, AkshayaGomathi K, Mahesh Velan S. Numerical Study on Parametric Analysis of Reinforced Concrete Column under Blast Loading. J Perform Constr Facil 2020;34:04019102. https://doi.org/10.1061/(asce)cf.1943-5509.0001382.
[37] Abedini M, Zhang C. Dynamic performance of concrete columns retrofitted with FRP using segment pressure technique. Compos Struct 2021;260:113473. https://doi.org/10.1016/j.compstruct.2020.113473.
[38] Abedini M, Zhang C, Mehrmashhadi J, Akhlaghi E. Comparison of ALE, LBE and pressure time history methods to evaluate extreme loading effects in RC column. Structures 2020;28:456–66. https://doi.org/10.1016/j.istruc.2020.08.084.
[39] Rebelo HB, Cismasiu C. A Comparison between three air blast simulation techniques in LS-DYNA. 11th Eur LS-DYNA Conf Salzburg, DYNAmore Https//Www Dynalook Com/Conferences/11th-European-Ls-Dyna-Conference/Air-Blast-2/a-Comparison-between-Three-Air-Blast-Simulation-Techniques-in-Ls-Dyna/View 2017.
[40] Schwer L. A Brief Introduction to Coupling Load Blast Enhanced with Multi-Material ALE: The Best of Both Worlds for Air Blast Simulation. Ger LS-DYNA Forum 2010:1–12.
[41] UNIFIED FACILITIES CRITERIA (UFC) STRUCTURES TO RESIST THE EFFECTS OF ACCIDENTAL EXPLOSIONS. 2008.
[42] Tabatabaei ZS, Volz JS. A Comparison between Three Different Blast Methods in LS-DYNA®: LBE, MM-ALE, Coupling of LBE and MM-ALE. 12th Int LS-DYNA Users Conf 2012:1–10.
[43] Gholipour G, Zhang C, Mousavi AA. Numerical analysis of axially loaded RC columns subjected to the combination of impact and blast loads. Eng Struct 2020;219. https://doi.org/10.1016/j.engstruct.2020.110924.
[44] Abedini M, Mutalib AA, Raman SN, Baharom S, Nouri JS. Prediction of Residual Axial Load Carrying Capacity of Reinforced Concrete (RC) Columns Subjected to Extreme Dynamic Loads. Am J Eng Appl Sci 2017;10:431–48. https://doi.org/10.3844/ajeassp.2017.431.448.
[45] BAKER WE, WESTINE PS, DODGE FTBT-FS in E, editors. 4 - Scaling of Air Blast Waves. Similarity Methods Eng. Dyn., vol. 12, Elsevier; 1991, p. 49–69. https://doi.org/https://doi.org/10.1016/B978-0-444-88156-4.50010-5.

[46] Esparza ED. Blast measurements and equivalency for spherical charges at small scaled distances. Int J Impact Eng 1986;4:23–40. https://doi.org/https://doi.org/10.1016/0734-743X(86)90025-4.
[47] Fallah AS, Louca LA. Pressure-impulse diagrams for elastic-plastic-hardening and softening single-degree-of-freedom models subjected to blast loading. Int J Impact Eng 2007;34:823–42. https://doi.org/10.1016/j.ijimpeng.2006.01.007.
[48] Hao H, Stewart MG, Li Z, Shi Y, Engineering R. RC Column Failure Probabilities.pdf 2010;1:571–91.